

*Non-contact detection and identification of blood stained
fingerprints using visible wavelength reflectance hyperspectral
imaging: part 1*

Abstract

Blood is one of the most commonly encountered types of biological evidence found at scenes of violent crime and one of the most commonly observed fingerprint contaminants. Current visualisation methods rely on presumptive tests or chemical enhancement methods. Although these can successfully visualise ridge detail, they are destructive, do not confirm the presence of blood and can have a negative impact on DNA sampling.

A novel application of visible wavelength reflectance hyperspectral imaging (HSI) has been used for the detection and positive identification of blood stained fingerprints in a non-contact and non-destructive manner on white ceramic tiles. The identification of blood was based on the unique visible absorption spectrum of haemoglobin between 400 and 680 nm.

HSI has been used to successfully visualise ridge detail in blood stained fingerprints to the ninth depletion. Ridge detail was still detectable with diluted blood to 20 fold dilutions. Latent blood stains were detectable to 15,000 fold dilutions. Ridge detail was detectable for fingerprints up to six months old. HSI was also able to conclusively distinguish blood stained fingerprints from fingerprints in six paints and eleven other red/brown media with zero false positives.

Keywords

Fingerprints, Blood detection, Forensic Science, Hyperspectral Imaging

Abbreviations

DS- Detect stain

DSLR- Digital single lens reflex

HSI- Hyperspectral imaging

PRD- Partial ridge detail

UV- Ultraviolet

WRD- Whole ridge detail

Contents

1. Introduction.....	4
2. Material and Methods	5
2.1 Contamination of digit	5
2.2 HSI system- Version 1	6
2.3 HSI system- Version 2	6
2.4 Hyperspectral reflectance image acquisition and pre-processing	6
2.5 Criteria for the identification of blood stains	6
2.6 Grading of fingerprints.....	6
2.7 DSLR setup	7
2.8 Trials.....	7
2.8.1 Depletions	7
2.8.2 Dilutions.....	8
2.8.3 Other contaminants	8
2.8.4 Detection of aged blood stained fingerprints	8
3. Results and Discussion	8
3.1 Depletions.....	9
3.2 Dilutions	9
3.3 Other contaminants	10
3.4 Detection of aged blood stained fingerprints	11
4. Conclusion	12

1. Introduction

Blood is one of the most commonly encountered types of biological evidence found at scenes of violent crime [1] and is the most commonly observed fingerprint contaminant [2].

The first challenge for examiners when dealing with blood evidence is to establish that the substance is blood before performing further analysis [3]. Even for experienced examiners some blood stains can be missed or confused with other substances. The misidentification of blood can lead to lost time, mislead investigations and wasted resources in carrying out potentially expensive follow up analyses, such as DNA analysis. The current forensic workflow involves visual examination followed by chemical presumptive tests to indicate the presence of blood [2]. Whilst these chemical tests can be very sensitive, they are not specific to blood and can generate false positives [2]. Additionally these chemical tests may contaminate the stain, leading to dilution and alteration of the shape of the stain as well as potentially affecting subsequent DNA analysis [4]. Because of these issues examiners normally test areas only when they suspect blood evidence is present but cannot be visually identified, due to problems detecting latent (not visible) stains or stains on dark backgrounds. Fingerprints contaminated with blood are subject to chemical enhancement methods, such as acid stains, including Acid Black 1, Acid Violet 17 or Acid Yellow 7 [2]. Although these techniques can successfully visualise ridge detail, they have a number of drawbacks. They can be destructive, as incorrect application of the enhancement process will result in a loss of ridge detail [2] and there is a risk of background staining of the substrate obscuring any enhanced ridge detail. Also, successful enhancement of a blood stained fingerprint does not conclusively confirm the presence of blood and the staining process may interfere with subsequent recovery of DNA material from the fingerprint.

Previous studies exploring blood stain detection originally focused on blood typing [5] or the use of alternate light sources, such as ultraviolet light [6]; or high intensity light sources [7]. However the former requires considerable sample preparation and is destructive; and the latter both rely on minimal background interference. UV light could also affect subsequent DNA recovery, as DNA in biological samples can be degraded by ultraviolet light [8]. Other methods such as immuno-chromatographic analysis [9] or RNA analysis [10,11] have been successfully used to identify blood stains. These methodologies are destructive however, which is not suitable for blood stained fingerprints, where the aim is to confirm the contaminant is blood while preserving ridge detail.

Optical techniques, such as microscopic analysis have been used to confirm the presence of blood [12], although this approach has so far only been explored on lifts of microscopic blood stains. Spectroscopic methods have been used to determine the presence of blood through compositional analysis. Raman spectroscopy has been used with some success in controlled lab conditions, but there remain substrate interference challenges [13]. X-ray fluorescence spectroscopy was explored in terms of gunshot residue through a collaborative piece of research between the National Institute of Justice (NIJ) and the National Aeronautics and Space Administration's (NASAs) Goddard Space Flight Centre (GSFC) [14]. Blood was successfully identified through the presence of iron from haemoglobin, although this could be vulnerable to false positives with other substances with high iron concentrations.

More recently research has explored the use of non-contact reflectance spectroscopy to detect blood stains with high levels of specificity [15]. Blood was identified based on the spectral shape of the α and β bands in haemoglobin between 500 nm and 600 nm, and these bands were also used to estimate the age of the blood stains. Our group also reported a similar contemporaneous approach for the age estimation of blood stains using a microspectrophotometer [16].

Recent exploration of blood stain identification using near-infrared demonstrated significant advantages over visible light, particularly on dark coloured substrates [17,18], although the

spectral property of other protein-containing substances can be similar to blood resulting in false positives [3]. Other work has explored the visible region using forensic photography. One study successfully used a background correction technique to improve the detection of blood stains on coloured and patterned substrates [19], although the sensitivity was not as high in comparison to existing presumptive tests.

Over the last couple of years visible wavelength hyperspectral imaging has been reported for firstly the age determination of blood stains [16,20] and also the detection of blood stains using the α and β bands between 500 nm and 600 nm [21-23]. The methods proposed allowed for rapid, non-destructive presumptive blood stain detection. Most recently our group has proposed a new blood stain identification approach based on hyperspectral imaging and the use of the Soret γ band absorption in haemoglobin [3]. This was shown to provide a higher sensitivity and specificity for the detection and identification of blood stains over previously proposed methods.

There is to date a definite gap in previous research concerning the detection of blood stained fingerprints using non-contact and non-destructive methods. An ideal method should be highly sensitive and effective even with blood diluted to latent (not visible by the human eye) levels in both stains and fingerprints and should be highly specific to avoid false positives. The visible wavelength hyperspectral imaging method proposed in this paper meets all these requirements. In this study we present a novel application of visible wavelength hyperspectral imaging (HSI) based on the Soret γ band absorption in haemoglobin between 400 and 500 nm for the non-contact, non-destructive detection and identification of both blood stains and ridge detail in blood stained fingerprints on white tiles. This is the first time the detection of blood stained fingerprints has been explored using hyperspectral imaging and is potentially a significant step towards a reliable method for both non-destructive blood identification and the detection of ridge detail in blood stained fingerprints.

2. Material and Methods

2.1 Contamination of digit

Both human and horse blood were used as contaminants in this study. Human blood from a consenting healthy volunteer was used where the blood stains were to be analysed and disposed of within one day (trial 1). A sterile lancet (FinePoint, USA) in a Penlet Plus lancing device (LifeScan, USA) was used to pierce the left middle finger. The finger was gently squeezed to encourage blood flow and the resulting blood drops were evenly spread over the ridge detail on the right middle finger. In trials 2, 3 and 4 screened horse blood was used. This was deposited into a Petri dish containing a small sponge. The right middle finger was pressed against the sponge to evenly coat the digit and the blood stained fingerprint then deposited onto the substrate. For standard samples human and horse blood stained fingerprints were allowed to dry for approximately 1 hour before analysis. Wet samples were analysed within 20 minutes of deposition and dry samples were left to dry for 2 hours before analysis. Application of paints and other contaminants was carried out by applying a small quantity to a gloved left middle finger. The contaminant was then evenly spread over the ridge detail on the right middle finger and the fingerprint deposited. All white ceramic tiles (B&Q, UK) were cleaned with distilled water and thoroughly dried before labelling and fingerprint deposition.

2.2 HSI system- Version 1

The HSI system (*Version 1*) used in this study was similar to that detailed in [3], consisting of a liquid crystal tuneable filter (LCTF) coupled to a 2.3 megapixel Point Grey camera and a light source for scene illumination. The light source was comprised of two 40W LEDs; one violet giving an output at 410nm and one white, giving an output between 450 and 700 nm. Control of the LCTF and image capture was performed using custom developed software written in C++ (Microsoft, USA). Images were captured between 400 nm and 680 nm with spectral sub sampling at 5 nm intervals, resulting in an image cube at 56 wavelengths for each scan. Spectra from the image cube were subsequently analysed using custom routines developed in Visual Studio (Microsoft, USA) and Spyder (Python, USA). The time required to acquire and process an image was approximately 30 seconds.

2.3 HSI system- Version 2

An improved version of the HSI system (*Version 2*) was created using an upgraded camera and an improved liquid crystal tuneable filter (LCTF). The camera was a 5.5 megapixel CMOS pco.edge camera coupled to a Varispec CRI liquid crystal tuneable filter. The same lighting setup was used as detailed above in 2.2. Control of the LCTF and image capture was again performed using custom developed software written in C++ (Microsoft, USA), as detailed in 2.2.

2.4 Hyperspectral reflectance image acquisition and pre-processing

The hyperspectral reflectance measurements were made following the method detailed in [3]. A reference image (R_0) was obtained using a blank ceramic tile. This image was recorded in a 5 nm series of 56 discrete wavelengths between 400 nm and 680 nm. The sample image (R_s) was recorded at the same wavelengths under the same illumination conditions and integration time settings on the camera. The hyperspectral reflectance image (R) consisted of a data cube of 1280×1024 pixel values at 56 discrete wavelengths. Additional information regarding sample image processing can be found in [3].

2.5 Criteria for the identification of blood stains

The presence of haemoglobin in blood dominates the blood reflectance spectrum in the visible region [16,20]. The spectrum contains a strong narrow absorption at 415 nm called the Soret or γ band with two weaker and broader absorptions between 500 and 600 nm known as the β and α bands [3]. Due to the absorption in the blue part of the visible spectrum, the Soret band is responsible for giving blood its distinctive red colour. Other red substances also absorb in the blue region of the visible spectrum between 400 and 680 nm. However, the width of these absorption features is typically much broader and also not centred at 415 nm. This forms the basis of the methodology to identify and discriminate blood stains from other similarly coloured substances. Further information is detailed in [3]. From the reflectance images obtained, the pixels which satisfied the criterion were marked as black, whilst all other pixels were marked as white. This allowed regions of the image where the blood stained fingerprint was present to be identified, as well as clear distinction of the ridge detail.

2.6 Grading of fingerprints

Fingerprint grading for trials involving 6 or 12 print depletion series was assessed based on three factors- the furthest deposition where it was possible to detect second level ridge detail

(eg. bifurcations, ridge endings) across the whole of fingerprint (whole ridge detail, WRD), where it was possible to detect some second level ridge detail (partial ridge detail, PRD), and where it was possible to detect the blood stain but no ridge detail at any level could be resolved (detect stain, DS). Whole ridge detail was assigned a score of three, partial ridge detail a score of two, detecting the stain a score of one, and no visualisation a score of zero as shown in *Figure 1*.

This grading method was used by the same experienced investigator for all fingerprints to compare the sensitivity of the techniques. The further down the depletion series ridge detail could be detected across the whole fingerprint, the higher the sensitivity of the technique. A single individual was used to grade all fingerprints, so as to remove the additional variable of subjective grading from different individuals. Fingerprints were graded from the on screen images generated by the custom software following hyperspectral analysis and the DSLR images copied from the memory card.

[Insert Figure 1]

Figure 1: Grading scale used for comparing the visualisation of second level ridge detail in blood stained fingerprints and the overall fingerprint stain between techniques, with example hyperspectral images for each grading score

2.7 DSLR setup

The images used in this report were taken using a digital single lens reflex (DSLR) camera mounted on a Kaiser RS1 copy stand. The DSLR was a Canon EOS 700D which was fitted with a Canon Angle Finder C 90° viewfinder with a 1.25-2.5x optical magnification and a Canon TC-80N3 remote control external shutter release to avoid camera motion. Images were taken using two sizes of macro lenses- a 50mm lens for overview shots of the substrates and a 100mm lens for high magnification macro shots of individual fingerprints. The lenses used were a Canon EF 50mm f2.5 macro lens and a Canon EF 100mm f2.8L macro IS USM lens. Substrates were lit using oblique lighting from two Daylight Twist Portable Lamps with a white light output of 6500K. Images were captured in aperture priority mode with an aperture of f/8 to ensure clarity of focus across the whole fingerprint and an ISO between 100 and 400 to minimise noise or grain in the images. The lighting setup in combination with the selected DSLR camera settings were determined in preliminary studies where clear second level ridge detail could be observed. DSLR images were saved onto a SanDisk 16GB memory card and transferred to a PC for grading.

2.8 Trials

Four trials were designed to explore fingerprint detection and realisation of ridge detail using both HSI setup *Version 1* and *Version 2* in comparison to ridge detail visible by DSLR. All fingerprints were deposited by one male donor (age 26, omnivore, no cosmetics).

2.8.1 Depletions

A depletion series of 12 fingerprints in undiluted human blood was deposited onto a white ceramic tile. The fingerprints were analysed using HSI (*Version 2*) to determine to which depletion ridge detail was still detectable.

2.8.2 Dilutions

Ten sets of six fingerprint depletions were deposited using horse blood diluted with distilled water (2 fold to 100 fold dilutions) onto white ceramic tiles and analysed using HSI (*Version 1*). The dilutions explored are shown in **Table 1**. Sample 10 was pure water as a control. The sensitivity of both HSI setups to detect diluted blood stains on white tiles was also explored using horse blood diluted with distilled water. The dilutions and corresponding blood concentrations with both setups (*Version 1* and *Version 2*) are also shown in **Table 1**. For both analyses 12 dilutions were deposited (10 μ L) onto white tiles and left to dry prior to analysis, as explained in **2.1**. Analysis of wet stains of the same dilutions was also carried out using HSI (*Version 1*).

[Insert Table 1]

Table 1: Dilutions of blood stained fingerprints and blood stains with ratio, fold dilution and estimated blood percentage concentration

2.8.3 Other contaminants

The ability of HSI to correctly distinguish fingerprints in blood was explored using commonly encountered red/brown contaminants with a very similar appearance to blood by eye. Six depletion series of 6 fingerprints were deposited using undiluted horse blood onto six white ceramic tiles. A 6 print depletion series using one of six red/brown water-soluble paints was then deposited onto each tile, as shown in **Table 2**, and the blood-paint pairs analysed using HSI. Additionally a single fingerprint contaminated with undiluted horse blood was deposited alongside 11 fingerprints contaminated with red/brown contaminants onto the same tile, as shown in **Table 2**, and analysed using HSI (*Version 1*).

[Insert Table 2]

Table 2: Red/brown paints and contaminants deposited alongside blood stained fingerprints

2.8.4 Detection of aged blood stained fingerprints

To ensure HSI detection and identification results were not adversely affected by fingerprint age, four fingerprints in undiluted horse blood were deposited onto a white ceramic tile and left to age under controlled conditions in an environmental chamber at 23-24°C (Qualicool LR202, LTE Scientific, UK). Contamination thickness was also explored. Two fingerprints were contaminated with a thick layer, consisting of five drops applied to the deposition finger. Two fingerprints were contaminated with a thin layer, consisting of one drop applied to the deposition finger. The fingerprints were aged under controlled conditions over 6 months. Both thick and thin fingerprints were analysed using HSI (*Version 1*) at 0 months and again after 1, 3, 4, 5 and 6 months. Longer time frames were not explored due to time restrictions.

3. Results and Discussion

The volume of human blood used was less than analyses involving horse blood, although comparisons are only reported between the same contaminant, where similar volumes were used (human with human, horse with horse).

3.1 Depletions

HSI detected whole and partial ridge detail to the 6th and 9th depletions respectively. The stain was still detected to the 12th depletion, although ridge detail was no longer observable, as shown in *Figure 2*. This was **better than DSLR photography**, as the same fingerprint viewed by DSLR showed whole and partial ridge detail only to the 5th and 7th depletions respectively. The stain was also observable to the 12th depletion.

[Insert Figure 2]

Figure 2: The 6th, 9th and 12th depletions on white tiles showing the HSI image (above) and by DSLR (below)

3.2 Dilutions

Previous research has demonstrated that HSI can be used to detect diluted blood stains up to 512 fold dilutions [3]. This was explored both for blood stains and blood stained fingerprints in this research and it was determined that there is considerable benefit to the use of HSI over DSLR, as shown in *Figure 3*. *Figure 3* shows the furthest deposition to which whole and partial ridge detail were detected as red and yellow bars respectively, for DSLR photography (9 bars on left) and HSI (9 bars on right). The green bars show at which depletion the stain could be detected with no ridge detail present.

Whole ridge detail was still observable to the second depletion in the hyperspectral image for blood stained fingerprints at a 5 fold dilution (HSI, red bar) compared to only a 3 fold dilution with DSLR (DSLR, red bar). Partial ridge detail was observable to the third depletion for blood stained fingerprints at a 5 fold dilution by DSLR (DSLR, yellow bar), whereas partial ridge detail was still present to the fourth depletion in the hyperspectral image at a 20 fold dilution (HSI, yellow bar).

Ridge detail was not observable for further dilutions due to the fluid nature of the contaminant preventing the deposition of ridges, making ridge detail visualisation impossible. Additionally, the presence of small bubbles in the blood-water mixture produced during mixing resulted in some ridge detail obscured for the initial deposition. This did not have a significant bearing on the overall results however. Sample 10, the pure water control, showed no ridge detail after HSI analysis as expected.

The stain with no ridge detail was only detected for the first depletion at a 100 fold dilution with DSLR (DSLR, green bar), compared to the fifth depletion with HSI (HSI, green bar). This demonstrates several advantages of HSI over DSLR, both due to the higher sensitivity identified in this comparison and the ability to positively discriminate for blood.

[Insert Figure 3]

Figure 3: Stacked bar graph showing the depletion to which whole ridge detail (WRD), partial ridge detail (PRD) and the stain only (DS) were detected for diluted blood stained fingerprints analysed by DSLR and HSI (Version 1)

Further diluted blood stains were explored to identify the limit of detection of both HSI setups. Analysis using HSI (*Version 1*), detected wet stains to 5000 fold dilutions, as shown in *Figure 4*. Dry stains were also detected to 5000 fold dilutions on white tiles, although there was considerable noise within the image. A 5000 fold dilution corresponds to 0.020% of the deposited material composed of blood. Each stain was composed of 10 μL of diluted blood, which equates to the HSI (*Version 1*) setup detecting around 2 nL of blood at 5000 fold dilution.

Analysis using HSI (*Version 2*) detected a clear blood stain at 5000 fold dilution, as shown in **Figure 5**. A more noisy image was obtained for a 7500 fold dilution, although the stain was still observable in the hyperspectral image. The stains at 10,000 and 15,000 fold dilutions were still detected, although the hyperspectral images were very noisy and the stain was less visible against the background. The stain for the 20,000 fold dilution was not detected. A 15,000 fold dilution corresponds to 0.0067% of the deposited material composed of blood. A 10 μ L stain of diluted blood was deposited, which equates to around 0.67 nL of blood at 15,000 fold dilution.

Overall the limit of detection for HSI (*Version 2*) is between 5000 fold and 15,000 fold for dry blood stains, due to increased levels of noise in the images at lower dilutions. However, this limit could be improved by increasing the exposure time, as that would increase the amount of light entering the camera and possibly improve the signal-to-noise ratio.

[Insert Figure 4]

Figure 4: Images of wet (top) and dry (bottom) diluted stains on white tiles: DSLR (left) and HSI (Version 1) images (right)

[Insert Figure 5]

Figure 5: Images of diluted (dry) stains on white tiles: DSLR (left) and HSI (Version 2) images (right)

3.3 Other contaminants

The ability to immediately identify whether a red/brown stain is blood is particularly useful. This study compared blood stained fingerprints against different shades of paint and a selection of red/brown contaminants commonly encountered at crime scenes.

HSI successfully distinguished all of the 6 red/brown paints compared against blood stained fingerprints, as shown in **Figure 6**, as only the blood stained fingerprint is displayed as black in the hyperspectral image. The other stains are not enhanced and appear white.

HSI also correctly identified the blood stained fingerprint compared to 11 deposited red/brown fingerprints, as shown in **Figure 7**. In the DSLR image it is difficult to identify which, if any, of the fingerprints are blood, whereas only the blood stained fingerprint in the processed hyperspectral image is displayed as black ridge detail against a white background. The blood stained fingerprint was therefore identified correctly. The lack of any enhanced ridge detail for the hyperspectral images for any of the eleven other contaminants demonstrates the accuracy of the setup at distinguishing blood from other contaminants. To date there have been zero false positives identified with either stains or fingerprints.

[Insert Figure 6]

Figure 6: The hyperspectral image (left) and the DSLR image (right) for blood stained fingerprints and fingerprints with 6 red/brown paint contaminants

[Insert Figure 7]

Figure 7: The hyperspectral image (left) and the DSLR image (right) for blood stained fingerprints and fingerprints with 11 red/brown contaminants

3.4 Detection of aged blood stained fingerprints

Analysis of blood stained fingerprints over 6 months yielded visible ridge detail for all thick and thin fingerprints from 0 months to 6 months. Ridge detail was still clearly observable in the thick deposits after 6 months, although ridge detail was slightly less visible in the centre of the thin deposits after 6 months, as shown in *Figure 8*. This is possibly due to the degradation of blood over time resulting in reduced absorption at the key wavelengths used to identify blood. Improvements to the HSI sensitivity, such as increasing the lighting intensity may solve this problem, although the majority of the ridge detail was still visible in the thin deposits so the slight loss of ridge detail is not a major concern.

[Insert Figure 8]

Figure 8: Blood stained fingerprints analysed using HSI (Version 1) over 6 months; thick (above) and thin (below) depositions

4. Conclusion

A novel implementation of visible wavelength reflectance hyperspectral imaging has been used for the non-contact and non-destructive detection and positive identification of blood stained fingerprints and blood stains on white ceramic tiles. In the processed hyperspectral images, pixels where blood was identified were coloured black whilst all other pixels were coloured white, thus enhancing the location of ridge detail in blood stained fingerprints.

This is the first time HSI has been used to visualise and conclusively identify both blood stains and blood stained fingerprints in a non-destructive and non-contact manner and demonstrates a potential considerable advantage over existing chemical enhancement methods, as HSI analysis is both non-contact and non-destructive, thereby minimising any damage to the ridge detail present. This also could remove the need for presumptive tests, which could destroy part of a sample and reduce the volume of material available for further forensic tests, such as DNA analysis. Using HSI, a blood stained fingerprint can be analysed and the blood positively identified within thirty seconds. This could be particularly beneficial for cases which require a rapid turnaround of forensic results or where there is considerable suspected blood evidence at a scene.

Further work is required to compare the effectiveness of HSI for the detection of blood stained fingerprints across a range of substrates, as well as against existing chemical enhancement methods, so as to explore the potential of implementing HSI within the existing forensic workflow for blood detection and identification. Results to date have shown zero false positives with non-blood contaminants, although additional red/brown contaminants including non-blood proteins need to be investigated, as well as a larger contaminants discrimination study with a range of coloured substrates to fully test the ability of the setup. The application of the technique for large scale analysis could be compared against current methods for the enhancement of suspected large scale blood stains, such as where blood evidence is suspected to span entire walls or rooms. Additionally, a comparison of the effectiveness of HSI both before and after chemical enhancement could demonstrate an additional potential application of the method as a non-contact rapid confirmatory technique following standard presumptive tests or chemical fingerprint enhancement methods. The images currently generated by the existing hyperspectral setup are not of sufficient resolution to allow for real-world comparison between fingerprints and crime scene marks, but planned improvements to the prototype should increase this resolution sufficiently. Improvements to the custom software should also allow for images from the HSI Version 2 setup to be more effectively compared.

Development of a more rugged instrument could lead on to a robust portable device which could be used at crime scenes. Additionally with further research and development HSI at ultraviolet wavelengths has the potential to be used to detect other biological material such as saliva, semen, and sweat, as well as latent natural fingerprints. Previous research exploring the age determination of blood stains could also be applied to blood stained fingerprints, which would allow for both the non-contact, non-destructive identification and visualisation of ridge detail and a determination of the age of the blood with which the fingerprint was deposited.

References

- [1] Jonathan Finnis, Jennie Lewis, Andrew Davidson, Comparison of methods for visualizing blood on dark surfaces, *Science & Justice*, 53, 2, (2013), 178-186
- [2] Home Office CAST, Fingerprint Sourcebook, Chapter 3, 3.1 Acid Dyes, 1st ed., Home Office, 2013
- [3] Bo Li, Peter Beveridge, William T. O'Hare, Meez Islam, The application of visible wavelength reflectance hyperspectral imaging for the detection and identification of blood stains, *Science & Justice*, 54, 6, (2014), 432-438
- [4] Neha Passi, Rakesh Kumar Garg, Mukesh Yadav, Ram Sarup Singh, Magdy A. Kharoshah, Effect of luminol and bleaching agent on the serological and DNA analysis from bloodstain, *Egyptian Journal of Forensic Sciences*, 2, 2, (2012), 54-61
- [5] Irmgard Oepen, Identification of characteristics in blood and semen stains — A review, *Forensic science international*, 36, 3-4, (1988), 183-191
- [6] G. Richardson, Ultraviolet, Infrared and Fluorescence, In E. Robinson, Crime Scene Photography, Academic Press, 2007, pp. 383-421
- [7] Milutin Stoilovic, Detection of semen and blood stains using polilight as a light source, *Forensic science international*, 51, 2, (1991), 289-296
- [8] Jacob Wawryk, Morris Odell, Fluorescent identification of biological and other stains on skin by the use of alternative light sources, *Journal of Clinical Forensic Medicine*, 12, 6, (2005), 296-301
- [9] Stefania Turrina, Giulia Filippini, Renzo Atzei, Elisabetta Zaglia, Domenico De Leo, Validation studies of rapid stain identification-blood (RSID-blood) kit in forensic caseworks, *Forensic Science International: Genetics Supplement Series*, 1, 1, (2008), 74-75
- [10] M. Bauer, RNA in forensic science, *Forensic Science International: Genetics*, 1, 1, (2007), 69-74
- [11] Kelly Virkler, Igor K. Lednev, Analysis of body fluids for forensic purposes: From laboratory testing to non-destructive rapid confirmatory identification at a crime scene, *Forensic science international*, 188, 1-3, (2009), 1-17
- [12] K. De Wael, L. Lepot, F. Gason, B. Gilbert, In search of blood—Detection of minute particles using spectroscopic methods, *Forensic science international*, 180, 1, (2008), 37-42
- [13] Gregory McLaughlin, Vitali Sikirzhytski, Igor K. Lednev, Circumventing substrate interference in the Raman spectroscopic identification of blood stains, *Forensic science international*, 231, 1-3, (2013), 157-166
- [14] Jacob I. Trombka, Jeffrey Schweitzer, Carl Selavka, Mark Dale, Norman Gahn, Samuel Floyd, James Marie, Maritza Hobson, Jerry Zeosky, Ken Martin, Timothy McClannahan, Pamela Solomon, Elyse Gottschang, Crime scene investigations using portable, non-destructive space exploration technology, *Forensic science international*, 129, 1, (2002), 1-9
- [15] Rolf H. Bremmer, Annemarie Nadort, Ton G. van Leeuwen, Martin J. C. van Gemert, Maurice C. G. Aalders, Age estimation of blood stains by hemoglobin derivative determination using reflectance spectroscopy, *Forensic science international*, 206, 1-3, (2011), 166-171
- [16] Bo Li, Peter Beveridge, William T. O'Hare, Meez Islam, The estimation of the age of a blood stain using reflectance spectroscopy with a microspectrophotometer, spectral pre-processing and linear discriminant analysis, *Forensic science international*, 212, 1-3, (2011), 198-204
- [17] Gerda Edelman, Vicky Manti, Saskia M. van Ruth, Ton van Leeuwen, Maurice Aalders, Identification and age estimation of blood stains on colored backgrounds by near infrared spectroscopy, *Forensic science international*, 220, 1-3, (2012), 239-244

- [18] Apollo Chun-Yen Lin, Hsing-Mei Hsieh, Li-Chin Tsai, Adrian Linacre, James Chun-I Lee, Forensic Applications of Infrared Imaging for the Detection and Recording of Latent Evidence, *Journal of forensic sciences*, 52, 5, (2007), 1148-1150
- [19] J. H. Wagner, G. M. Miskelly, Background correction in forensic photography I. Photography of blood under conditions of non-uniform illumination or variable substrate color - Theoretical aspects and proof of concept, *Journal of forensic sciences*, 48, 3, (2003), 593-603
- [20] Bo Li, Peter Beveridge, William T. O'Hare, Meez Islam, The age estimation of blood stains up to 30 days old using visible wavelength hyperspectral image analysis and linear discriminant analysis, *Science & Justice*, 53, 3, (2013), 270-277
- [21] Suwatwong Janchaysang, Sarun Sumriddetchkajorn, Prathan Buranasiri, Tunable filter-based multispectral imaging for detection of blood stains on construction material substrates Part 2: realization of rapid blood stain detection, *Applied Optics*, 52, 20, (2013), 4898-4910
- [22] Suwatwong Janchaysang, Sarun Sumriddetchkajorn, Prathan Buranasiri, Tunable filter-based multispectral imaging for detection of blood stains on construction material substrates Part 1: Developing blood stain discrimination criteria, *Applied Optics*, 51, 29, (2012), 6984-6996
- [23] G. J. Edelman, E. Gaston, T. G. van Leeuwen, P. J. Cullen, M. C. G. Aalders, Hyperspectral imaging for non-contact analysis of forensic traces, *Forensic science international*, 223, 1-3, (2012), 28-39

Table 1

Blood fingerprints (HSI Version 1)				Blood Stains (HSI Version 1)				Blood Stains (HSI Version 2)			
Number	Ratio	X Fold	% Concentration	Number	Ratio	X fold	% Concentration	Number	Ratio	X fold	% Concentration
1	1:0	Pure	100%	1	1:0	Pure	100.000%	1	1:0	Pure	100.0000%
2	1:1	2 fold	50%	2	1:9	10 fold	10.000%	2	1:9	10 fold	10.0000%
3	1:2	3 fold	33%	3	1:49	50 fold	2.000%	3	1:49	50 fold	2.0000%
4	1:3	4 fold	25%	4	1:99	100 fold	1.000%	4	1:99	100 fold	1.0000%
5	1:4	5 fold	20%	5	1:199	200 fold	0.500%	5	1:499	500 fold	0.2000%
6	1:9	10 fold	10%	6	1:499	500 fold	0.200%	6	1:999	1000 fold	0.1000%
7	1:19	20 fold	5%	7	1:999	1000 fold	0.100%	7	1:1999	2000 fold	0.0500%
8	1:49	50 fold	2%	8	1:1499	1500 fold	0.067%	8	1:4999	5000 fold	0.0200%
9	1:99	100 fold	1%	9	1:1999	2000 fold	0.050%	9	1:6499	7500 fold	0.0154%
10	0:1	0	0%	10	1:2999	3000 fold	0.033%	10	1:9999	10,000 fold	0.0100%
11	-	-	-	11	1:3999	4000 fold	0.025%	11	1:14999	15,000 fold	0.0067%
12	-	-	-	12	1:4999	5000 fold	0.020%	12	1:19999	20,000 fold	0.0050%

Table 2

CONTAMINANT	Red/Brown Paints	Other Contaminants
HUMAN BLOOD	✓	✓
RED OCALDO POSTER PAINT	✓	-
PAINT- LIGHT RED 362	✓	-
PAINT- ALIZARIN CRIMSON HUE 003	✓	-
PAINT- BURNT SIENNA 074	✓	✓
PAINT- BURNT UMBER 076	✓	✓
MIXED SIENNA AND UMBER RED PAINT	✓	✓
TOMATO KETCHUP	-	✓
COFFEE	-	✓
MILK CHOCOLATE	-	✓
FAKE BLOOD	-	✓
NAIL VARNISH- FISHNET STOCKINGS	-	✓
NAIL VARNISH- RUSSIAN ROULETTE	-	✓
LIP STICK- VINTAGE ROSE 13	-	✓
PARKER RED INK	-	✓

Figure 1

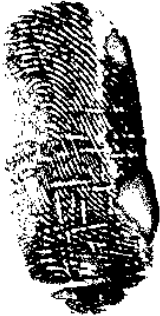
Observable second level ridge detail	Abbreviation	Grading Score	HSI Example Image
Whole ridge detail	WRD	3	
Partial ridge detail	PRD	2	
Detect stain only	DS	1	
No stain visible	-	0	

Figure 2

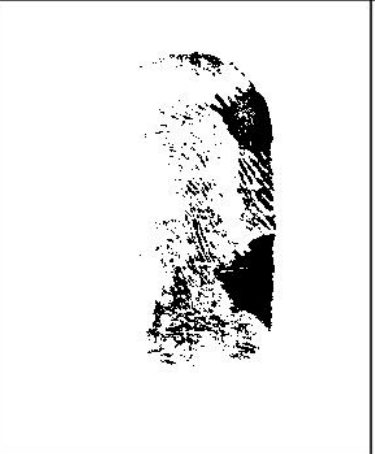
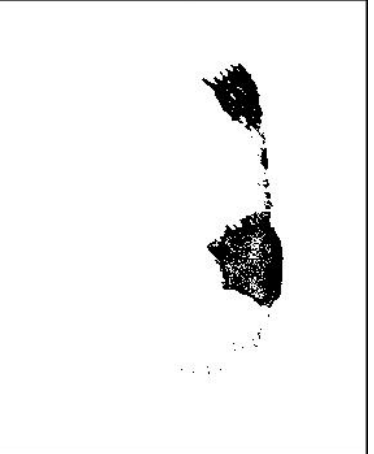
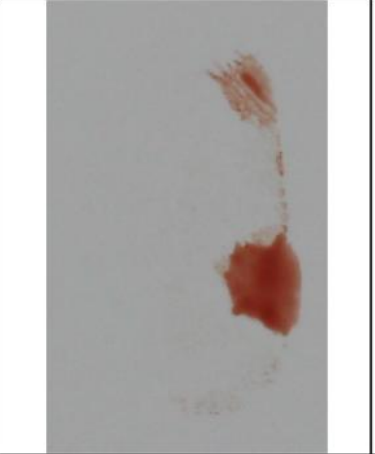
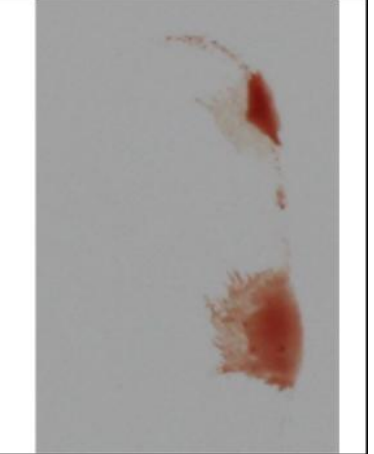
	6th Depletion	9th Depletion	12th Depletion
HSI			
DSLR			

Figure 3

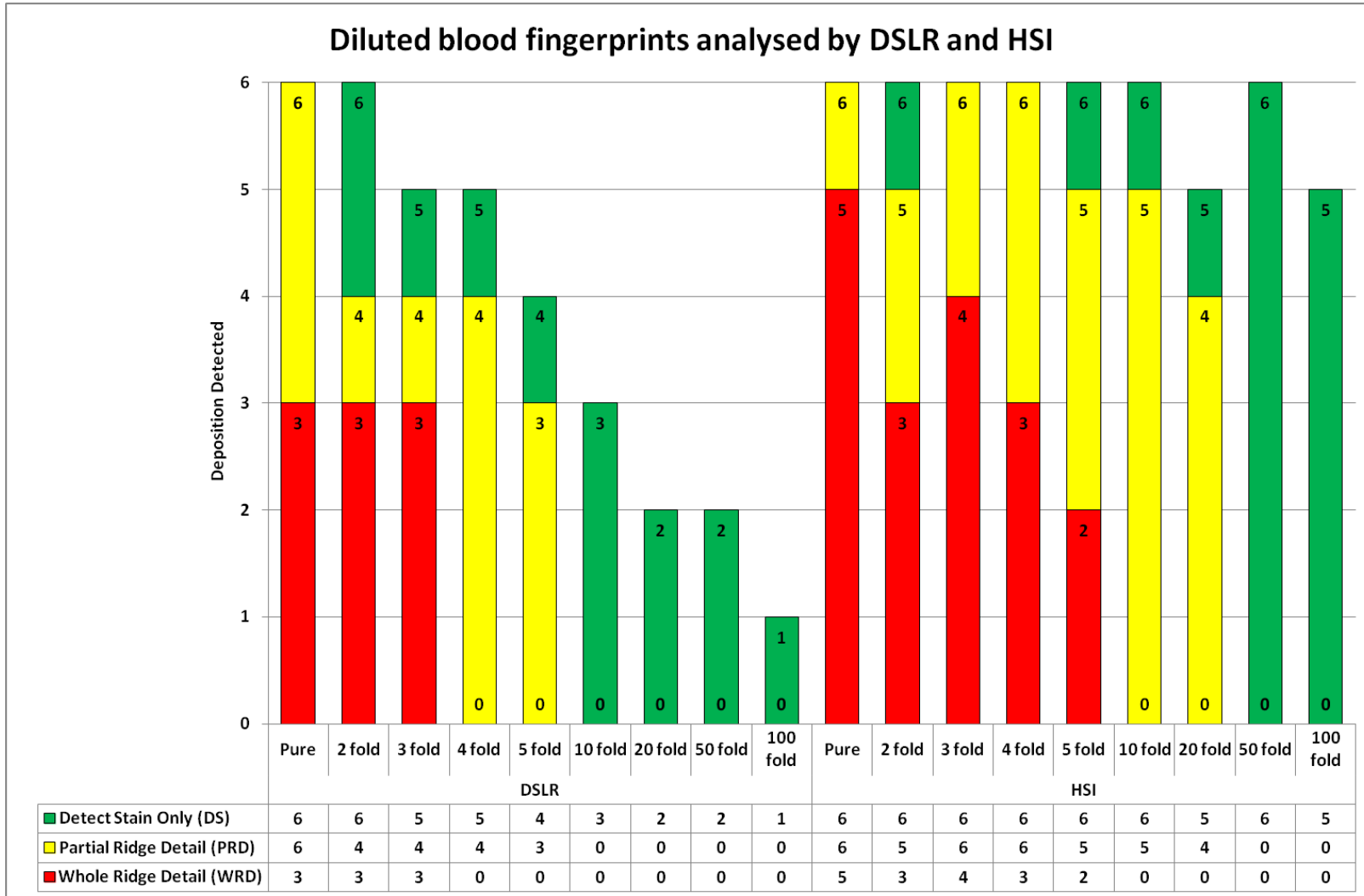


Figure 4

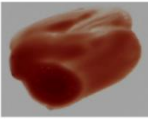
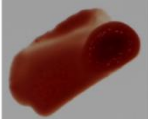
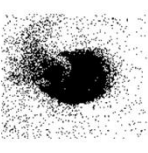
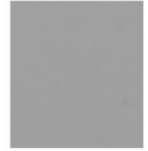
WET/DRY	DILUTION	DSLR	HSI
WET	PURE		
	10 FOLD		
	100 FOLD		
	1000 FOLD		
	5000 FOLD		
DRY	PURE		
	10 FOLD		
	100 FOLD		
	1000 FOLD		
	5000 FOLD		

Figure 5

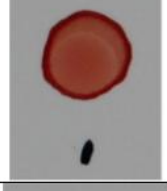
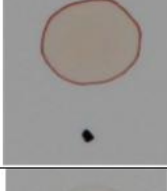
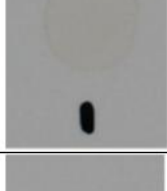
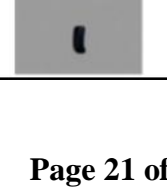
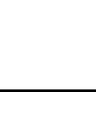
DILUTION	DSLR	HSI
PURE		
10 FOLD		
100 FOLD		
1000 FOLD		
5000 FOLD		
7500 FOLD		
10,000 FOLD		
15,000 FOLD		
20,000 FOLD		

Figure 6

	HSI	DSLR	
RED OCALDO POSTER PAINT			
LIGHT RED 362			
ALIZARIN CRIMSON HUE 003			
BURRNT SIENNA 074			
BURNT UMBER 076			
MIXED SIENNA AND UMBER RED PAINT			

Figure 7

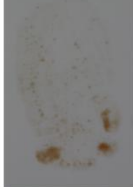
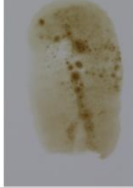
	HSI	DSLR		HSI	DSLR
BLOOD			MILK CHOCOLATE		
PAINT- BURNT SIENNA 074			FAKE BLOOD		
PAINT- BURNT UMBER 076			NAIL VARNISH- FISHNET STOCKINGS		
PAINT- MIXED PAINT			NAIL VARNISH- RUSSIAN ROULETTE		
KETCHUP			LIP STICK- VINTAGE ROSE 13		
COFFEE			PARKER RED INK		

Figure 8

	0 months	1 month	3 months	4 months	5 months	6 months
THICK						
THIN						